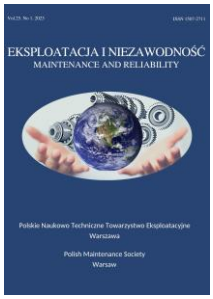

Eksploatacja i Niezawodnosc – Maintenance and Reliability

Volume 25 (2023), Issue 1

journal homepage: http://www.ein.org.pl

Article citation info:
Jabłońska M, Jurczak W, Ozimina D, Adamiak M, Increasing the operational reliability of a ship by using a composite impeller in the event of hydrophore pump failure. Eksploatacja i Niezawodnosc – Maintenance and Reliability 2023: 25(1) http://doi.org/10.17531/ein.2023.1.18

Increasing the operational reliability of a ship by using a composite impeller in the event of hydrophore pump failure

Indexed by: Web of Science Group

Monika Jabłońska[a*], Wojciech Jurczak[a], Dariusz Ozimina[b], Marcin Adamiak[c]

[a] Polish Naval Academy, Faculty of Mechanical and Electrical Engineering, Jana Śmidowicza 69 str., 81-127 Gdynia, Poland
[b] Kielce University of Technology, Faculty of Mechatronics and Mechanical Engineering, Tysiąclecia Państwa Polskiego 7 str., 25-314 Kielce, Poland
[c] Silesian University of Technology, Faculty of Mechanical Engineering, Materials Research Laboratory, Konarskiego 18A str., 44-100 Gliwice, Poland

Highlights

- The proposed composite impeller enables the pump to operate continuously, reliably and at maximum load for 48 hours.
- Optimum printing parameters enable the desired geometry of surface structure to be achieved.
- The flow, power and efficiency characteristics of the pump are consistent with the reference model.
- Carbon fibres, reinforcing the filament randomly distributed in the extrusion stage are arranged in parallel.

Abstract

The time-consuming technological process of manufacturing impellers and the high production costs are the reason for the search for alternative materials and manufacturing methods. In this paper, based on a literature analysis, the performance of a pump with an impeller that was manufactured by an incremental method from polyethylene terephthalate with an admixture of glycol and carbon fibre (PETG CF) was selected and studied. Operation tests were conducted on the ship's rotodynamic pump test bench. The composite impeller pump was shown to have an efficiency at the selected printing parameters of 26,23%, comparable to a tin bronze impeller, which has an efficiency of 27,7%. The maximum pump useful power with the impellers tested was 337 W at a flow rate of 4.42 m^3/h. The results confirm that, with a filament layer height of 0.12 mm and 100% fill in the four print contours, the pump characteristics obtained are consistent with those of the reference impeller. This fact ensures continuous operation of the ship's pump for 48 hours which makes the chosen manufacturing method a reliable emergency method of impeller repair in offshore operations.

Keywords
carbon-fibre reinforced polyethylene terephthalate glycol (PETG CF), ship's impeller, pump test bench, pump useful power, total pump efficiency, reliability, 3D printing

1. Introduction

Maintaining the operational reliability of a ship is one of the fundamental aspects that ensure the safety of the crew and the vessel. Failure of a part of a ship's mechanism at sea is a hazardous condition that requires repairs to be carried out more quickly, enabling, inter alia, a safe return to a port.

One of the most failure prone ship parts is the water pump impeller [16, 18]. It is one of the key elements on a ship, being not only an essential part of the ship's installation system, but also an indispensable component to enable vessels to carry out their assignments [9]. Due to the high failure rate of water pump impellers not only on ships, but also in other equipment requiring this part, operators and designers are considering possible technological improvements and changes in manufacturing methods to increase its reliability. In nanotechnology, the use of 3D printing has been proposed [7, 15, 22]which also solves the problem of the very small size of parts used. However, this technology does not need to be limited to nano-elements, and indeed it would be a waste not to research its effectiveness in terms of shipboard equipment.

However, this is associated with a number of challenges and constraints that the proposed solution must address. The main factor is the volume of space required for the process of making parts on the vessel. This space is limited and allows the printing of parts with dimensions of 170 × 170 × 170 mm. Another

(*) Corresponding author.
E-mail addresses: M. Jabłońska (ORCID: 0000-0003-4731-4034) m.jablonska@amw.gdynia.pl, W. Jurczak (ORCID: 0000-0003-1879-8084), w.jurczak@amw.gdynia.pl, D. Ozimina (ORCID: 0000-0001-5099-6342) ozimina@tu.kielce.pl, M. Adamiak (ORCID: 0000-0001-8851-2091) marcin.adamiak@polsl.pl

attribute is the harsh environmental conditions. Ambient temperature is variable and depends on time of day, year, latitude. The technology must therefore be dimensionally stable under large temperature fluctuations [26]. Moreover, it shall be stressed that the occurring vibration, rolling and pitching along with accompanying phenomena, which force the application of another boundary condition, i.e. stabilisation during the manufacture of the part [24]. An important point is the ease of use of the printer in question, which should be at such a level that the vessel's crew can use it for printing without undergoing specialised training. The last condition is that there is no finishing treatment after the print stage of the component, so that the geometric structures of the surface are obtained.

Traditional impeller manufacturing technology is complex and expensive. This process includes rough machining (casting, forging, rolling, etc.) and a finishing stage (milling, drilling, grinding, turning, cutting, etc.). To ensure that these processes are carried out, support systems such as water, electricity, compressed air must also be provided [13]. Traditional impeller manufacturing technology is uneconomical and needs to be adapted to a sustainable development strategy. Its main pillars are innovation, care for the environment, management of materials, waste or the reduction of production costs.

The answer to these challenges is the use of 3D printing technology on board of the vessel, i.e. the printing of a composite replacement, which will enable the equipment to be temporarily repaired while maintaining similar operating parameters, which shall enable safe return of a ship to the port without any support. Sea hydrometeorological conditions were assumed to be up to sea state 3 on Beaufort wind force scale. Tilt stabilisers will be used during part printing.

There are many 3D printing technologies available: directed energy deposition (DED) [3, 20], stereolithography (SLA) [17, 21], selective laser sintering (SLS) [11, 17], fused deposition modelling (FDM) [8, 12, 17, 25], electron beam melting (EBM) [23].

Analysing the constraints and assumptions associated with the choice of printing technology, i.e. no finishing, printer size, ability to maintain dimensional stability with large temperature fluctuations, low costs, stability during printing, ease of handling or availability of materials, it was decided to choose fused deposition modelling (FDM). The technique is an additive process. Printed models are created by applying successive layers of thermoplastic material extruded from a nozzle, following a G-code path generated by the printer's control software. This software maps the desired geometry of the part. The extrusion nozzle is heated to the melting point of the material. It can move horizontally and vertically. The material is supplied in the form of filament (fixed-diameter strands of 1,75 mm or 2,85 mm) wound on a reel or pellets which are fed from a hopper. The filament can be located in different places in the printer. It is essential for the filament to be supplied continuously to the extruder and the printer head.

The chosen 3D printing technology has many advantages, such as the ability to print complex geometries, the use of innovative materials, [2]reduction of machining waste, reduction of manufacturing and [5] and storage costs, [14] reduced production and prototyping times.

2. Materials and methods

During the tests, the operating parameters of the SKA.5.01 circulating rotodynamic pump were determined, in which a impeller replacement manufactured in a short time on a 3D printer was used. The tests, which lasted for several months, allowed for the selection of such printing parameters and the selection of such filaments for the adopted manufacturing method so that printing would be possible under shipboard conditions, in the shortest possible time. The mentioned pump is used on ships as a hydrophore pump of fresh or sea water (fig. 1) and performs the following functions: pumping liquids through the ship's installations, emptying ballast tanks, draining bilges of ship's holds and engine rooms, supplying water to boilers, pumping sea water, fresh water, oils and chemically non-aggressive liquids [4, 19]. The main working element of this pump is the blade impeller (fig. 2) mounted on a rotating shaft. During operation, the impeller blades exert pressure on the fluid and force it to flow in the ducts between the blades from the impeller's operating axis towards its outer diameter [6]. Due to the occurrence of cavitation and high loads to which the impeller is subjected during operation, it is often subject to damage. The reference pump impeller is made by casting in tin bronze.

Fig. 1. SKA 5.01 hydrophore pump used in shipboard installations (part of test rig) [own materials].

Fig. 2. Appearance of a shipboard pump impeller made using tin bronze casting technology [own materials].

The impeller replacement was printed on a 3D printer from polyethylene terephthalate with an admixture of glycol and carbon fibre (PETG CF). The selection of the filament was based on a multi-criteria analysis and testing of the mechanical properties and moisture absorption of the filament. Higher tensile and bending strength, high impact strength, low water absorption are characteristic of this material. It is designed to operate in extreme conditions. The filament contains reinforcement material in the form of short carbon fibres ,(approximately 15%), which are randomly distributed in the frame. The fibres contain over 90% of elemental carbon and have diameters in the range of five to ten micrometres. The microstructure of this reinforced filament is shown in fig. 3.

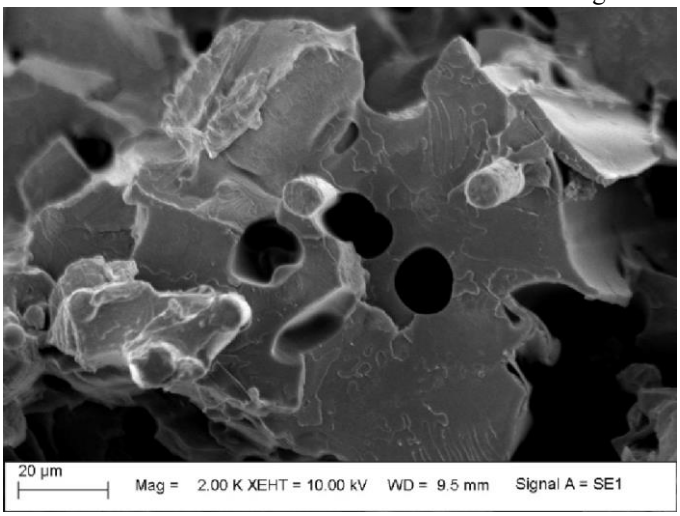

Fig. 3. Microstructures of carbon fibres located in a bond of polyethylene terephthalate with an admixture of glycol and carbon fibre (PETG CF) of the tested impeller number 3 after 48 h of operation at maximum load. Microstructure (×2000) [own materials].

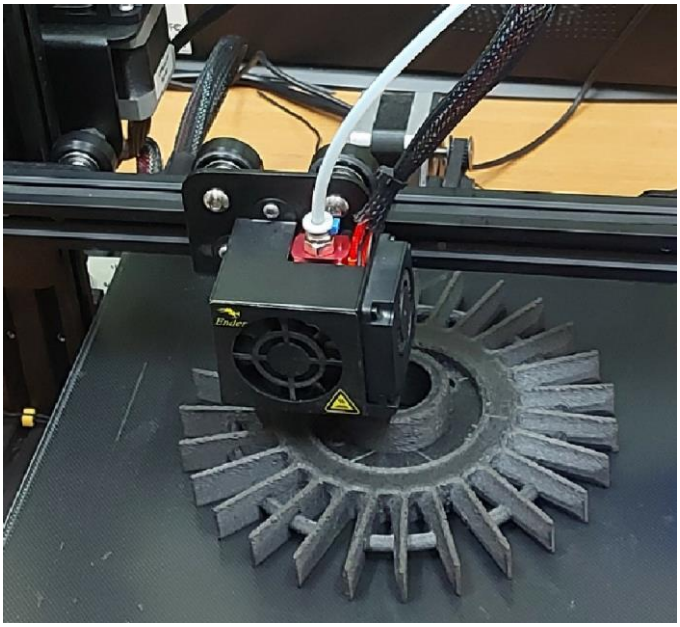

Fig. 4. Final stage of FDM impeller fabrication [own materials].

The parameters that were used to manufacture the tested impellers from the PETG CF material are summarised in table 1, and figure 4 illustrates the final stage of 3D printing one of several impellers tested.

Table 1. 3D printing parameters used when printing pump impellers

Impeller number	Filling percentage %	Layer height mm	Number of outlines -	Table temp. °C	Nozzle temp. °C
1	100	0.2	3	70	260
2	100	0.2	4	70	260
3	100	0.12	4	70	260

The tests were carried out at the ship's rotodynamic pump test bench located at the Ship Engine Room Operation Laboratory of the Naval Academy (LESO) showed on fig. 5. The test and measurement bench comprised: a pumping unit, a main circulating water tank with a volume of 9 m^3, a water measuring tank with a volume of 0,2 m^3, a system of pipelines, valves, measuring instruments: e.g. a flow meter with a Hall sensor, pressure sensors, temperature sensor, an optical sensor of rotational speed of an electric motor.

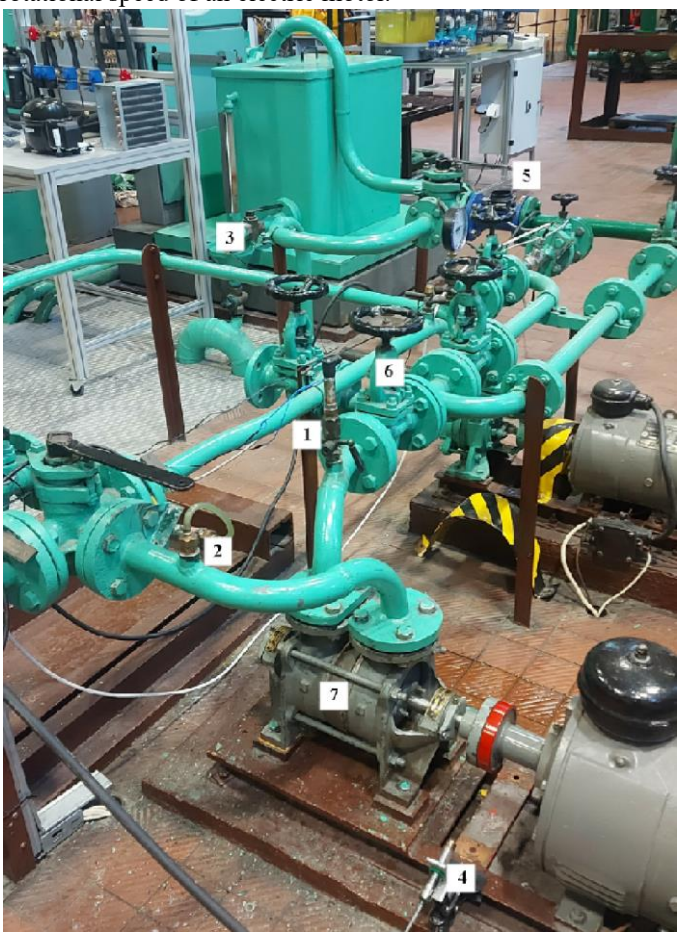

Fig. 5. Pump test bench (LESO) and diagram of the location of the sensors for the main operating parameters of the centrifugal pump. (1) discharge pressure sensor, (2) suction pressure sensor, (3) temperature measurement, (4) optical engine speed sensor, (5) flow meter with Hall sensor, (6) setpoint valve, (7) SKA 5.01 pump [own materials].

The tests on the test bench presented above, the pump head (H) and fluid flow rate (Q) were determined at a constant 1450 rpm of the drive motor. The change of pump capacity was realised by a throttling valve with manual setpoint. The operation parameters were recorded using a Metronics Instruments multi-channel recorder. Table 2 summarises the

parameters that were registered during the experimental tests.

Table 2. Summary of the registered operating parameters of the LESO pump test bench.

Channel number	Function
01	Discharge pressure measurement, bar
02	Suction pressure measurement, bar
09	Discharge water temperature, °C
17	Motor speed, rpm
18	Flow rate, m^3/h

The determined performance characteristics of the pumps with the original and modified impellers covered the entire operating range of the pump (from minimum to maximum load) and included ten measurement points determined by the position of the control valve, over a range of water discharge pressures from 0.1 MPa to 0.4 MPa, in 0.05 MPa increments. Readings of individual measured parameters were taken every 15 minutes after the new balanced state was defined. The set parameters were adjusted by varying the position of the angle setpoint in the discharge pipeline.

3. Findings

The pump performance values determined during the experimental tests:

- Pump useful power,

defined as useful power determined experimentally by measuring the effective pump head H_u and the flow rate Q. For formula (1) defining the pump useful power, the density of water was taken as a function of temperature according to the MST 1990 international temperature scale.

$$P_u = Q\rho g\, H_u \tag{1}$$

where:

Q – flow rate, m^3/s,

ρ – density of the fluid flowing through the pump, kg/m^3,

g – acceleration due to gravity, m/s^2,

H_u – pump discharge useful height, m.

The characteristic curve relates to one rotational speed equal to 1450 rpm. The test was carried out in triplicate for each load, each measuring point being the average of 10 measurements. The load time for a given discharge pressure was 15 minutes.

Table 3 shows the results of the tests determining the useful power of the pump, using the original reference metallic impeller b-c and 1, 2, 3 – the non-metallic impeller.

Fig. 6 illustrates the power parameters of the pump under test from its capacity $P = f(Q)$. The non-metallic impellers labelled 1, 2, 3 differed in their fabrication parameters (see table 1) which showed that the greatest discrepancy in results with respect to the tin bronze reference impeller occurred in impellers 1 and 2. The power characteristics of the described impeller number 3 corresponded to those of reference impeller. The highest useful power was gained by the impeller number 3. This was due to the fact that when printing the impeller, the 0,12 mm height of the filament layer and four outlines were applied. Reducing the height of the filament layer allowed for an increase in the mapping accuracy of the printed component, resulting in power characteristics that correlated with those of the tin bronze impeller.

Table 3. Useful power of the tested pump when using impellers of different materials: Tin bronze impeller b-c, impeller 1 ÷ 3 carbon-fibre reinforced polyethylene terephthalate glycol.

Discharge pressure *MPa*	Average useful power P_u *W*			
	Impeller b-c	*Impeller 1*	*Impeller 2*	*Impeller 3*
0.009	114	102	103	115
0.1	246	212	211	241
0.125		231	227	269
0.15		244	238	290
0.175		250	243	306
0.20	327	251	242	317
0.25		243	229	337
0.30	335	206	194	336
0.35		155	138	319
0.4	286	72	111	291

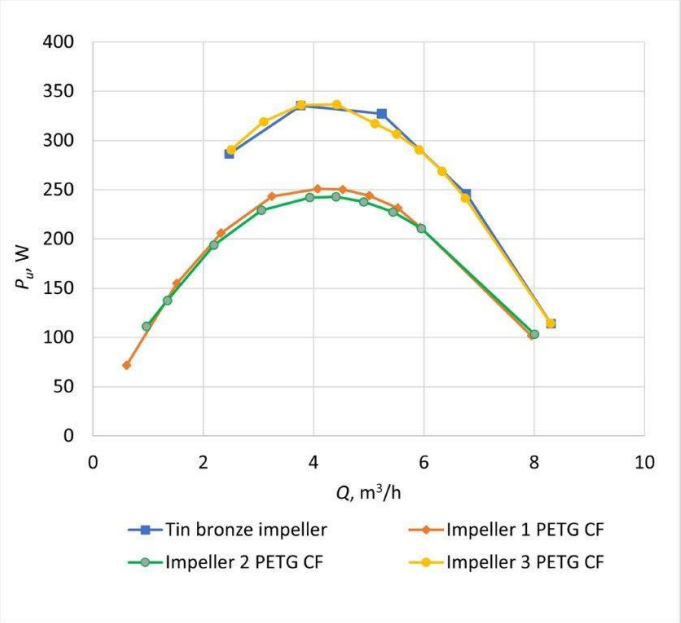

Fig. 6. Power characteristics of the centrifugal pump P = f(Q) using reference impeller 1 - made of tin bronze and replacements 1, 2, 3 - made of PETG CF

- Total pump efficiency

The total pump efficiency is defined as the ratio of the pump useful power (P_u) to the power delivered to the shaft *(P)*. The 4.8 kW PRDZc 160MC DC electric motor from Kolmec was used for the tests. The shaft power was calculated from relation (2), the motor efficiency was assumed to be 0,95.

$$\eta_0 = \frac{P_u}{P_w} = \frac{P_u}{P_{el}\eta_{sil}}, \tag{2}$$

where:

P_u – pump useful power, W,

P_w – power supplied to the shaft, W,

P_{el} – electrical power drawn from the grid, W,

$_{sil}$ – efficiency of the electric motor, 1.

Table 4 summarises the results of the performance tests for the overall efficiency of the DC motor-driven pump.

Table 4. Total efficiency of the tested pump when using impellers made of the following materials:
Tin bronze impeller b-c, impeller 1 ÷ 3 – carbon-fibre reinforced polyethylene terephthalate glycol.

Discharge pressure *MPa*	Average total pump efficiency η_0 *%*			
	Impeller b-c	*Impeller 1*	*Impeller 2*	*Impeller 3*
0.009	14.1	12.6	14.1	12.6
0.1	24.9	24.2	24.1	21.1
0.125		25.2	24.7	24.3
0.15		25.0	24.2	25.3
0.175		24.1	23.2	26.3
0.20	28.0	22.8	21.8	26.9
0.25		19.9	18.5	26.0
0.30	23.4	15.1	14.1	23.6
0.35			9.0	20.4
0.4	16.5	4.3	6.5	17.1

The results of the performance tests for the determined overall efficiency of the tested pump with different impellers are shown in fig. 7. Pump efficiency characteristic = *f*(Q) is a parabola with vertex (Q_{opt}, $_{opt}$). For the reference tin bronze impeller, the efficiency was 27,7% at the capacity of 5,29 m^3/h, for the non-metallic impeller number three the efficiency was 26,23% at the capacity of 5,1 m^3/h, while impellers 1 and 2 had similar values: efficiency 24,26% at the flow rate of 4,91 m^3/h. Higher efficiency of the impeller 3 by approximately 2% compared to the impellers 1 and 2 results , inter alia, from the smaller surface roughness of the composite impeller elements that pump the water. This surface condition is the result of the use of a lower filament layer height during printing – impeller no. 3.

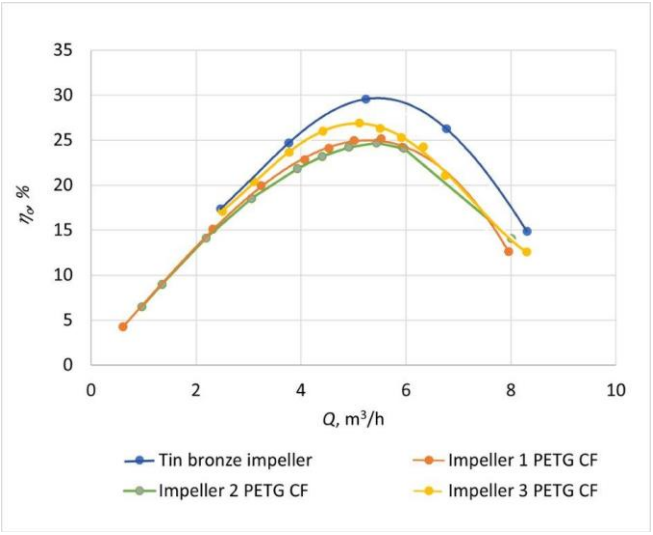

Fig. 7. Characteristics of the centrifugal pump = *f(Q)* with the use of: reference impeller – tin bronze impeller and replacements 1, 2, 3 made of PETG CF

- Pump flow characteristics

The flow characteristic *H* = f(*Q*) in the centrifugal pump shown in fig. 8 was determined for a nominal impeller (shaft) speed of 1450 rpm and a fixed impeller outer diameter of 148 mm. By throttling the control valve of the pump head H, the flow rate changed – was increasing. The throttling curve is stable.

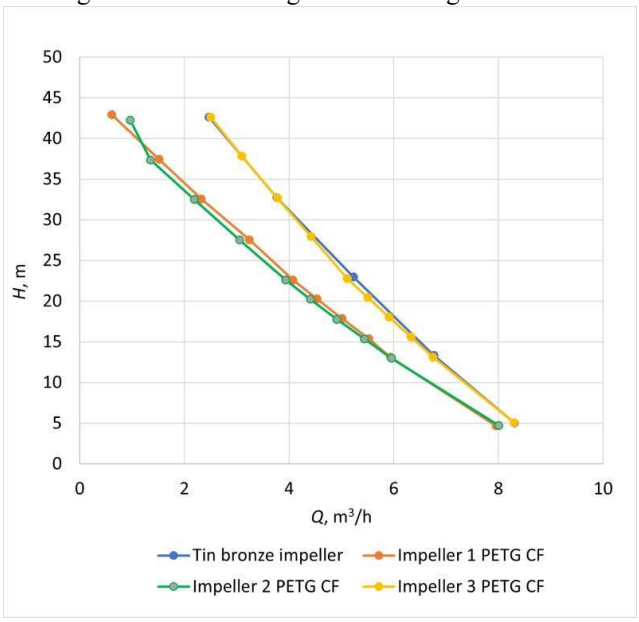

Fig. 8. Characteristics of the centrifugal pump flow *H* = *f(Q)* with the use of: reference impeller – tin bronze impeller and replacements 1, 2, 3 made of PETG CF

4. Testing the material structures of impellers made of PETG CF

After a phase of long-term research, the right printing parameters were selected for the PETG CF filament and a material with the best properties was obtained. Further analyses of the microstructures were carried out for a single material, and the structures developed relate only to the degree of degradation of the impeller structural surface dependent on the time of the test cycle.

On the basis of macro- and micro-structure studies performed on a Zeiss Supra 35 scanning microscope, the fractures of impeller material samples produced by 3D printing with PETG CF before and after certain stages of operation were described.

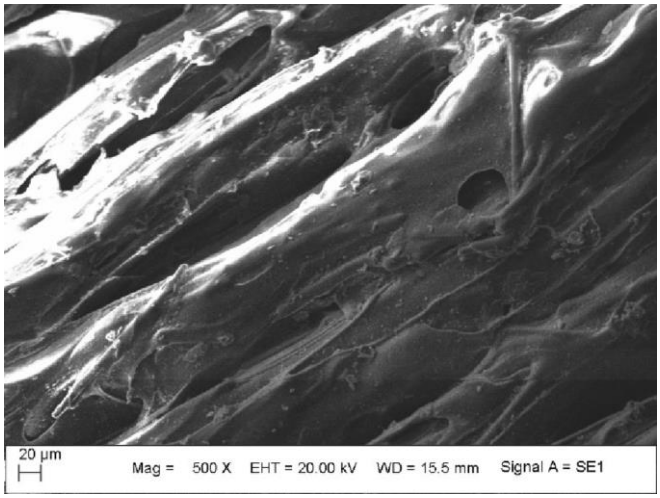

Fig. 9. Output microstructure of carbon fibre-reinforced PETG CF filament of the produced impeller no. 3 by FDM before experimental testing. Microstructure (×500). Experimental tests on the pump test bench included a test of the parameters of the SKA 5.01 centrifugal pump for the various stages of the test cycle differing in load parameters [own materials].

Figure 9 (impeller no. 3) indicates successive layers of filament, which are arranged in parallel against each other, but also intermingle in places. The carbon fibres are adhesively bonded to the frame and lay parallel to the print path, creating one way reinforcement. The diameter of the fibres is 10 micrometres, the length of a single fibre is approximately 144 micrometres.

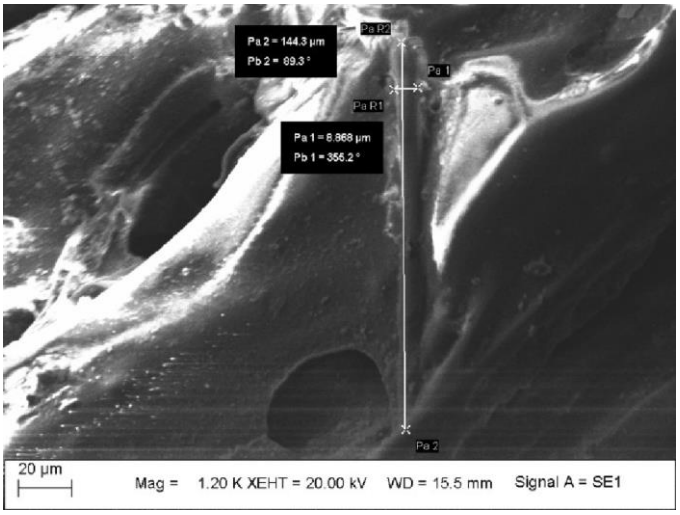

Fig. 10. Microstructure of carbon fibre-reinforced PETG CF filament of the produced impeller no. 1 by FDM after 8 hours of testing cycle. Microstructure (×1200) [own materials].

Figure 10 shows the microstructure of test impeller no.1 after an 8-hour test cycle at a magnification of 1200. Micro voids in the matrix are visible, indicating degradation of the impeller surface.

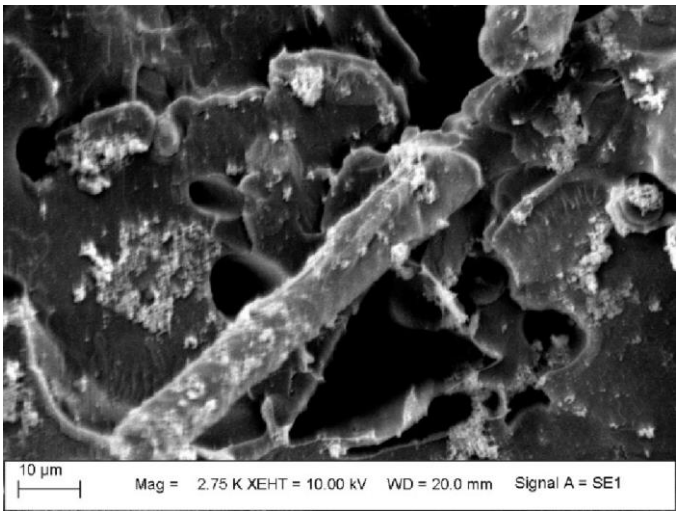

Fig. 11. Microstructure of carbon fibre-reinforced PETG CF filament of the produced impeller no. 1 by FDM after 8 hours of testing cycle. Microstructure (×2750) [own materials].

Figure 11, which was obtained using a magnification of 2750, shows carbon fibres that have been coated with a polymer build-up. Numerous pores were also observed, which are areas where fibres have been pulled out of the matrix during impeller operation. This is due to the low interfacial forces between the polymer matrix and the carbon fibres. Tested microstructure of fabricated impeller no. 1 by FDM after an 8-hour test cycle.

Figure 12 shows the microstructure of impeller no. 3 after the 48 h operating stage. It is noted that some of the fibres are above the surface of the matrix, and numerous fibre pores are also visible. Polymer build-up on the fibre surface is invisible, making it possible to conclude that, as the number of hours operated on a given sample increases, the fibre surface becomes smoother. On the other hand, the adhesive bond between the frame and fibres decreases with increasing operation time.

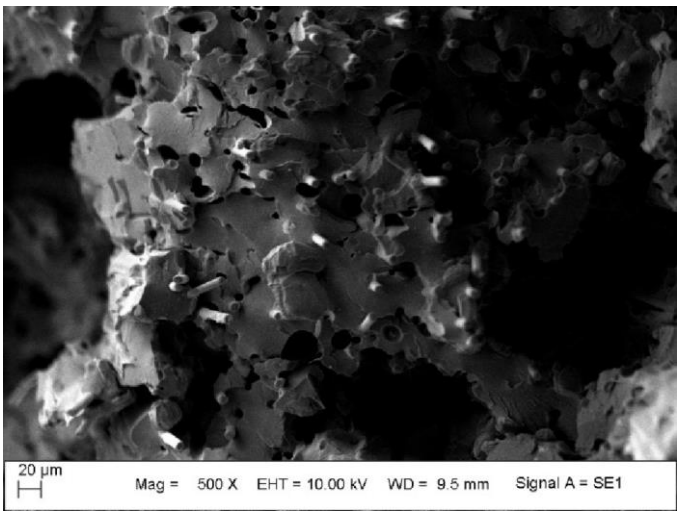

Fig. 12. Microstructure of carbon fibre-reinforced PETG CF filament of the produced impeller no. 3 by FDM after 48 hours of testing cycle. Microstructure (×500) [own materials].

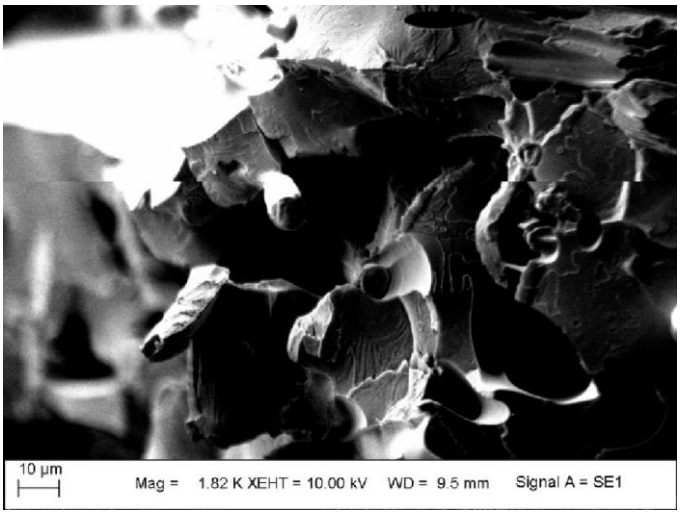

Fig. 13. Microstructure of carbon fibre-reinforced PETG CF filament of the produced impeller no. 3 by FDM after 48 hours of testing cycle. Microstructure (×1820) [own materials].

Figure 13 illustrates the microstructure of impeller no. 3 after a time of 48 h using a magnification of 1820. Exposed carbon fibres, numerous voids are visible. The carbon fibre breaks are irregular, indicating cavities and degraded surface condition.

5. Analysis of research results

A number of factors affects the correct operation of the pump. It is crucial to choose the right operating parameters for its optimum performance, depending on the medium to be transferred, such as temperature, pH, water hardness, fluid conductivity, but also on the operating power, head, nominal shaft speed, efficiency.

Table 5 summarises the operation time – testing cycle of the composite impellers and the operating parameters during which they failed.

Degradation of the surface of impeller no. 1 made of PETG CF occurred after 8 h 23 min. Operation parameters of the pump:

discharge pressure 0,35 MPa, flow rate 1.52 m^3/h, pump head 37.45 m The printing used a layer height of 0.2 mm, a sample volume fill density of 100% and 3 outer layers of the printed impeller.

Impeller no. 2 failed while the pressure in the discharge line was 0,25 MPa, a flow rate of 3.08 m^3/h, pump head of 27.54 m, and a water temperature of 19,48°C. When printing this impeller, the parameter for the number of outer layers was changed, increasing it by one, while keeping the previous printing parameters unchanged. The operation cycle of impeller 2 was 7 h 51 min.

Impeller no. 3 has worked as many as 48 hours and 23 minutes with a discharge pressure 0,4 MPa and a pump head of 42.72 m. Such favourable operating characteristics of the above impeller are due to the correct determination of the parameters of the printing. The filling used was 100%, layer height 0,12 mm, as well as the applied 4 outlines to form the contour of the model. The test bench temperature was 70°C, temperature of the printing nozzle 260°C. The reproduction of the impeller model geometry during printing was correct.

Table 5. Summary of test cycle parameters from the pump test bench of composite impellers fabricated by FDM with PETG CF

Impeller	Printing time	Operation time	Discharge pressure measurement *MPa*	Suction pressure measurement *MPa*	Discharge water temperature *°C*	Flow rate m^3/h	Pump head *m*
1	13:55:35	08:23:03	0.35	-0.018	18.86	1.52	37.45
2	13:52:50	07:51:03	0.25	-0.020	19.48	3.08	27.54
3	21:56:24	48:21:02	0.4	-0.018	17.97	2.5	42.72

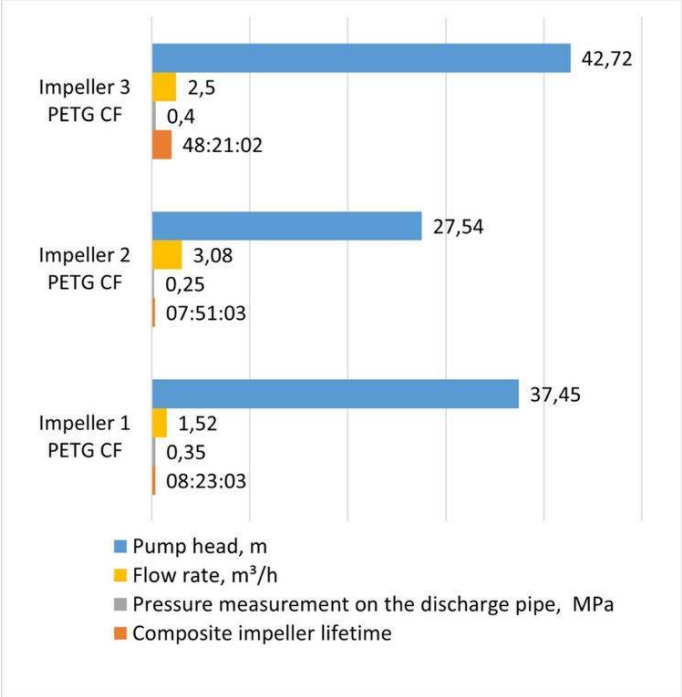

Fig. 14. Pump reliability graph for operating parameters, during which a pump failure has occurred (impeller failure)

The bar chart (fig. 14) illustrates the parameters during which the composite impellers failed. The data included: composite impeller lifetime, pump head, flow rate and pressure measurement on the discharge pipe. The longest operation life of 48 h 21 min was obtained by composite impeller no. 3, which used the lowest extruded layer height, i.e. 0.12 mm, and 4 contours to form the model shell. The lifespan of impellers 1 and 2 was about 73% shorter and this was due to the 0.2 mm layer height used and fewer contours during 3D printing.

The highest pump head of 42.72 m at a flow rate of 4 bar was achieved by impeller no. 3. This result was 55% higher than impeller 2 and 14% higher than impeller 1.

6. Discussion

Equipment failure is one of the greatest challenges facing current manufacturing technology. Despite the use of modern solutions and good quality materials, manufactured components often cannot meet expectations in terms of reliability or durability, which is why it is important to search for and research new methods and materials [9]. However, this is a major challenge, given the aforementioned enormity of the requirements that the proposed materials must meet.

3D printing represents a huge opportunity for designers due to the relatively low cost of producing prototypes, allowing for an expansion of research into the use of this technology. In addition, in 3D printing, it is very easy to make modifications to the designed part through changes to the 3D model. This enables faster and less costly testing of new components, as well as work on their geometry, which increases their efficiency [1, 10].

3D printing technology is, therefore, a very interesting and effective method, offering a range of possible materials with different properties, which undoubtedly makes it worthy of further research not only in the field of shipbuilding, but many other areas of life.

7. Conclusions

The in-service testing of the SKA 5.01 pump with FDM impellers made from PETG CF concluded that:

1. Impeller number 3 has completed over 48 hours of continuous operation, under full load i.e. 0,4 MPa discharge pressure. This period allows the vessel to return safely to port in the event of pump impeller failure.
2. Correctly selected printing parameters, i.e. the height of the filament layer of 0.12 mm, four outlines, 100% filling, allowed to obtain operating characteristics of the pump similar to those using a tin bronze impeller.
3. Scanning electron microscopy tests confirmed the presence of carbon fibres as declared by the filament manufacturer. The fibres in the filament improved the mechanical properties and also increased the lifespan of the composite impellers.
4. Examination of the fractures of the specimens showed degradation of the material with increasing service life (numerous pores, fibres outside the contour of the matrix, polymer growths on the surface of the carbon fibres).
5. Carbon fibres were shown to be oriented in the direction of flow during extrusion.
6. The average pump useful power when using a tin bronze impeller was 286 W, 0,4 MPa discharge pressure. Using an impeller made of PETG CF

material, a higher average useful power output was obtained which reached 291 W.

7. The overall efficiency of the pump when using a tin bronze impeller was 16.5%. The use of additive manufactured impeller also resulted in a comparatively higher pump efficiency value, i.e. 17.1%.
8. In the future, it is envisaged that the geometric surface structure will be improved by applying PVD and CVD ceramic coatings during the surface treatment of the composite impeller, which will enable the operation time of the hydrophore pump to be extended.

References

1. Asomani S N, Yuan J, Wang L et al. Geometrical effects on performance and inner flow characteristics of a pump-as-turbine: A review. Advances in Mechanical Engineering 2020. doi:10.1177/1687814020912149, https://doi.org/10.1177/1687814020912149.
2. Barletta M, Gisario A, Mehrpouya M. 4D printing of shape memory polylactic acid (PLA) components: Investigating the role of the operational parameters in fused deposition modelling (FDM). Journal of Manufacturing Processes 2021; 61: 473–480, https://doi.org/10.1016/j.jmapro.2020.11.036.
3. Dutta B, Froes F H. Additive Manufacturing Technology. Additive Manufacturing of Titanium Alloys, Elsevier: 2016: 25–40, https://doi.org/10.1016/B978-0-12-804782-8.00003-3.
4. Górski Zygmunt, Perepeczko Andrzej. Pompy okrętowe. Gdynia Studium Doskonalenia Kadr S.C. WSM: 1996.
5. Gunaydin K, Türkmen H. Common FDM 3D Printing Defects. International Congress on 3D Printing (Additive Manufacturing) Technologies and Digital Industry. 2018.
6. Jędral W, Politechnika Warszawska, Oficyna Wydawnicza. Pompy wirowe. Warszawa, Oficyna Wydawnicza Politechniki Warszawskiej: 2014.
7. Joswig L, Vellekoop M J, Lucklum F. Miniature 3D-Printed Centrifugal Pump with Non-Contact Electromagnetic Actuation. Micromachines 2019; 10(10): 631, https://doi.org/10.3390/mi10100631.
8. Kun K. Reconstruction and Development of a 3D Printer Using FDM Technology. Procedia Engineering 2016; 149: 203–211, https://doi.org/10.1016/j.proeng.2016.06.657.
9. Lu Z X. Study and Development on Safety Operation of Marine Pump. Advanced Materials Research 2013; 734–737: 2681–2684, https://doi.org/10.4028/www.scientific.net/AMR.734-737.2681.
10. Malik A, Zheng Q, Zaidi A A, Fawzy H. Performance Enhancement of Centrifugal Compressor with Addition of Splitter Blade Close to Pressure Surface. Journal of Applied Fluid Mechanics 2018; 11(4): 919–928. https://doi.org/10.29252/jafm.11.04.28658
11. Muzaffar A, Ahamed M B, Deshmukh K et al. 3D and 4D printing of pH-responsive and functional polymers and their composites. 3D and 4D Printing of Polymer Nanocomposite Materials, Elsevier: 2020: 85–117, https://doi.org/10.1016/B978-0-12-816805-9.00004-1.
12. Novakova-Marcincinova L, Novak-Marcincin J, Barna J, Torok J. Special materials used in FDM rapid prototyping technology application. 2012 IEEE 16th International Conference on Intelligent Engineering Systems (INES), 2012: 73–76, https://doi.org/10.1109/INES.2012.6249805.
13. Ponticelli G S, Tagliaferri F, Venettacci S et al. Re-Engineering of an Impeller for Submersible Electric Pump to Be Produced by Selective Laser Melting. Applied Sciences 2021; 11(16): 7375, https://doi.org/10.3390/app11167375.
14. Rinaldi M, Caterino M, Manco P et al. The impact of Additive Manufacturing on Supply Chain design: a simulation study. Procedia Computer Science 2021; 180: 446–455, https://doi.org/10.1016/j.procs.2021.01.261.
15. Ruiz C, Kadimisetty K, Yin K et al. Fabrication of Hard–Soft Microfluidic Devices Using Hybrid 3D Printing. Micromachines 2020; 11(567): 567, https://doi.org/10.3390/mi11060567.
16. Sheikh A K, Younas M, Matar D, Al-Anazi D. Weibull analysis of time between failures of pumps used in an oil refinery. 2003.
17. Siemiński P, Budzik G, Politechnika Warszawska, Oficyna Wydawnicza. Techniki przyrostowe: druk drukarki 3D. Warszawa, Oficyna Wydawnicza Politechniki Warszawskiej: 2015.
18. Singh D, Suhane D A, Thakur M K. The Study of Failure Analysis of Centrifugal Pump on the Basis of Survey. 2013; 4(6): 3.
19. Smith D W, Crawford J, Moore P S. Marine Auxiliary Machinery. Elsevier: 2016.
20. Svetlizky D, Das M, Zheng B et al. Directed energy deposition (DED) additive manufacturing: Physical characteristics, defects, challenges, and applications. Materials Today 2021: S1369702121001139, https://doi.org/10.1016/j.mattod.2021.03.020.
21. Voet Vincent S. D., Strating T., Schnelting Geraldine H. M. et al. Biobased Acrylate Photocurable Resin Formulation for Stereolithography 3D Printing. ACS Omega 2018 3 (2), 1403-1408, https://doi.org/ 10.1021/acsomega.7b01648
22. Vyatskikh, A., Delalande, S., Kudo, A. *et al.* Additive manufacturing of 3D nano-architected metals. Nature Communications 9, 593 (2018). https://doi.org/10.1038/s41467-018-03071-9
23. Wang P, Sin W, Nai M, Wei J. Effects of Processing Parameters on Surface Roughness of Additive Manufactured Ti-6Al-4V via Electron Beam Melting. Materials 2017; 10(10): 1121, https://doi.org/10.3390/ma10101121.
24. Wełnicki W. Mechanika ruchu okrętu. Gdańsk, Politechnika Gdańska: 1989.
25. Yang, Y., Chen, Y., Wei, Y. *et al.* 3D printing of shape memory polymer for functional part fabrication. The International Journal of Advanced Manufacturing Technology 84, 2079–2095 (2016). https://doi.org/10.1007/s00170-015-7843-2
26. Ziółkowski M, Dyl T. Possible Applications of Additive Manufacturing Technologies in Shipbuilding: A Review. Machines 2020; 8(4): 84, https://doi.org/10.3390/machines8040084.